International Journal of Signal Processing, Image Processing and Pattern Recognition
Vol. 6, No. 4, August, 2013

# Source Localization in Shallow Ocean Using a Compressively Sampled Vector Sensor Array

N Suresh Kumar[1], Dibu John Philip[2], A. Unnikrishnan[3], C. Bhattacharya[4]
[1]*Naval Physical and Oceanographic Laboratory, Kochi 682021, India*
*Email: sureshkumarnpol@yahoo.co.in*
[2]*Rajagiri School of Engineering and Technology, Kochi 682039, India*
[3]*Naval Physical and Oceanographic Laboratory, Kochi 682021, India*
[4]*Defense Institute of Advanced Technology, Pune 411025, India*

**Abstract**

*Coastal surveillance and harbour defence are the most complex and challenging operational issues for modern navy in the current turbulent global political climate. In most of the coastal surveillance and harbour defence systems, long sea-bed arrays consisting of hundreds of pressure sensors are deployed along the coastal belt to capture the low frequency components emanating from the sub-surface targets. Deployment of these sensor-arrays along with its associated signal conditioning hardware at the ocean-bed is a challenging task. The output of the sensor-array is to be conditioned and then digitized using multi-bit analog to digital converters (ADC). Further, the digitized channel data are required to be send to a base station through a radio frequency link. In this paper, we propose a compressively sampled (CS) architecture of acoustic vector sensor (AVS) array, to estimate the direction of arrival (DoA) of multiple acoustic sources, in a range independent shallow ocean using a one-dimensional search without prior knowledge of the ranges and the depths of the sources. We extend the high resolution angular spectral estimators MUSIC, MVDR and subspace intersection method (SIM) to suit the compressively sampled AVS array architecture operating in a shallow ocean environment. This architecture promises a significant reduction in the number of sensors, analog signal conditioning hardware, data rate or bandwidth, the number of snapshots and the software complexity, leading to easy installation and maintenance.*

**Keywords:** *Acoustic vector sensor array, Coastal surveillance, Compressive sampling, Subspace intersection method.*

## 1 Introduction

High resolution bearing estimation or direction of arrival (DoA) estimation is one of the primary problems in coastal surveillance and harbour defence systems to protect the coastal resources. The demands of these challenges are growing, which requires effective surveillance to detect incursions from underwater, accurate determination and characterisation of the threat, the provision of suitable deterrence and, ultimately, the launch of an appropriate neutralising response. All this has to be taken care of in a very short time window.

Traditionally, the passive surveillance approach comprises of deploying long, uniform or multi-octave linear arrays of scalar pressure sensors, at the bottom of the ocean to localize

the low frequency components emanating from sub-surface targets. Multi-octave array structure provides constant beamwidth across the octave bands. Usually a large number of sensors are used to improve the array gain or directivity index of the array. Each sensor in the array is associated with its own front-end signal conditioning hardware consisting of a pre-amplifier, programmable gain amplifier, anti-aliasing filter and an ADC. The digitized output from the array is transmitted to the base-station through a RF link. The deployment of long arrays along with its front-end hardware at the ocean bottom is a complex task involving huge cost and effort. Therefore, any reduction in the number of sensors, front-end circuitry, data rate or bandwidth, drastically reduces the investment. Also, any reduction in the number of snapshots (time samples) to localize an underwater threat significantly improves the anti-submarine warfare strategic performance.

In this paper, an efficient seabed array architecture, which greatly reduces the complexity of the waterside security (WSS) system is proposed. The new architecture utilizes a compressively sampled acoustic vector sensor array, along with high resolution spatial processing algorithms modified for compressive spatial filtering in a shallow ocean environment, where the plane wave acoustic propagation model assumption is not valid.

An acoustic vector sensor provides complete characterization of the acoustic field at a point in space through simultaneous measurement of the tri-axial components of the particle velocity along with the scalar acoustic pressure. In order to reduce the number of sensors, an AVS array is used which requires roughly $\frac{1}{4}^{th}$ the number of sensors [1] compared to the traditional scalar pressure sensor array to achieve the same localization performance. Though an AVS array utilizes lesser number of sensors, the major issues to be addressed in conjunction with AVS array deployment for a given localization performance are; (1) number of channels and the associated analog hardware remains same as that of the pressure sensor array. This is due to the fact that, an AVS simultaneously measures three orthogonal components of the particle velocity along with the scalar acoustic pressure and hence each AVS provides 4 channels, (2) transmission data rate through RF link and the size of the spatial correlation matrix remains same as that of pressure sensor array. Thus, it is noteworthy that, though an AVS array drastically reduces the number of sensors, the number of channels and the associated signal conditioning hardware, transmission data rate, and spatial correlation matrix dimension remains same as that of pressure sensor array for achieving a bearing performance.

The applications of compressed sensing was initiated by Donoho [2] and Candes et al. [3] in the year 2006. Compressive sampling is a method to recover a sparse signal vector from very few non-adaptive, linear measurements by convex optimization [3, 4, 5], greedy algorithms [6, 7] or combinatorial algorithms [8, 9]. Compressive array processing algorithms presented in [10, 11] assumes the plane wave acoustic propagation model, which is not suitable for the sea-bed array deployed in shallow ocean supporting multi-modal acoustic wave propagation. High resolution spectral estimation array processing algorithms tailored for shallow ocean application, namely NM-MUSIC, NM- MVDR [12, 13] and SIM [14] requires a $4N \times 4N$ sample correlation matrix estimated from the array observation data vector $\in \mathbb{C}^{4N\times 1}$. In [15], the authors have shown the advantage of compressively sampling a vector sensor array considering a plain wave model. In this paper, we attempt to unify three frameworks to realize a hardware efficient seabed array architecture:- vector sensor array, compressed sensing and compressive spatial filtering algorithms, for high resolution bearing estimation of multiple acoustic sources in shallow ocean.

Outline of the paper is as follows. In section 2, we present the AVS array measurement

model for a horizontally stratified, range independent shallow ocean. Review of compressive sensing, benefits of the compressive sensing on AVS array processing and compressive sampling on AVS array is discussed in section 3. High resolution angular spectral estimation algorithms tailored for the compressively sampled AVS array operating in the shallow ocean is described in section 4. Simulation results and discussions are detailed in section 5. Finally, section 6 contains our conclusions.

## 2 AVS array data model for shallow ocean

The AVS array data model for shallow ocean, derived in [14] is used. Consider a uniform horizontal AVS array of $N$ sensors at depth $z$. The scenario under consideration is shown in Figure 1.

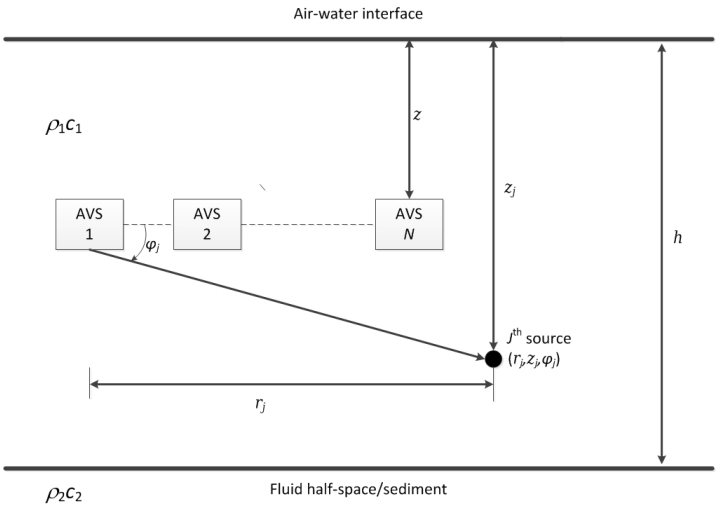


**Figure 1: Source and receiver array geometry.**

$\rho_1$ and $\rho_2$ are the densities of the water and the sediment/fluid half space respectively; while $c_1$ and $c_2$ are the sound speeds in water and sediment/fluid half space respectively. The array signal vector due to a source of unit strength at range $r_j$, depth $z_j$ and bearing $\phi_j$ with respect to the end-fire direction of the array when there are $M$ modes propagating, is given by

$$\mathbf{s}_j = \mathbf{A}(\phi_j)\mathbf{b}(r_j, z_j), \tag{1}$$

for $j$=1,...,$J$, where $J$ is the number of sources, $\mathbf{A}(\phi_j)$ is the array manifold matrix and $\mathbf{b}(r_j, z_j)$ is the modal pressure vector. Expressions for $\mathbf{A}(\phi_j)$ and $\mathbf{b}(r_j, z_j)$ are given by

$$\mathbf{A}(\phi_j) = [\mathbf{a}_1(\phi_j), \ldots, \mathbf{a}_M(\phi_j)], \tag{2}$$

$$\mathbf{a}_m(\phi_j) = \mathbf{c}_m(\phi_j) \otimes \mathbf{d}_m(\phi_j), \tag{3}$$

$$\mathbf{c}_m(\phi_j) = [1, e^{ik_m dcos\phi_j}, \ldots, e^{i(N-1)k_m dcos\phi_j}]^T, \tag{4}$$

where $\otimes$ denotes the Kronecker product, $d$ is the inter-sensor spacing and $k_m$ the wave-number of the $m$-th mode; for $m$=1, 2, ..., $M$. Now,

$$\mathbf{d}_m(\phi_j) = [1, \sqrt{2}\xi_m \cos(\phi_j), \sqrt{2}\xi_m \sin(\phi_j), \frac{-i\Psi_m(z)'}{k\Psi_m(z)}]^T, \tag{5}$$

$$\Psi_m(z) = sin(m\gamma z), \tag{6}$$

$$\gamma = \frac{\pi}{h_e}, \tag{7}$$

where the parameter $h_e$ is the frequency-dependent 'effective' depth of the water column. Also,

$$\xi_m(\phi_j) = \frac{k_m}{k} = \frac{k_m c}{2\pi f}, \tag{8}$$

$$\mathbf{b}(r_j, z_j) = [b_1(r_j, z_j), \ldots, b_M(r_j, z_j)], \tag{9}$$

$$b_m(r_j, z_j) = B\psi_m(z)\psi_m(z_j)e^{ik_m r_j - \delta_m r_j}. \tag{10}$$

Let $\eta_j(t)$ be the slowly varying complex amplitude of the signal from the $j$-th source at time $t$. The amplitudes $\eta_j(t)$, $j$=1, ..., $J$, are modelled as jointly stationary and uncorrelated circular complex narrow-band Gaussian random processes with mean zero and variance $\sigma_j^2 = E[|\eta_j(t)|^2]$. The array data vector inclusive of the received signals from all sources and the i.i.d circular complex random noise can be written as

$$\mathbf{y}(t) = \mathbf{S}\boldsymbol{\eta}(t) + \mathbf{w}(t), \tag{11}$$

where $\mathbf{S} = [\mathbf{s}_1, \ldots, \mathbf{s}_J]$, $\boldsymbol{\eta}(t) = [\eta_1(t), \ldots, \eta_J(t)]^T$, $\mathbf{w}(t) = [w_1(t), \ldots, w_{4N}(t)]^T$ and $w_1(t), \ldots, w_{4N}(t)$ are the i.i.d circular complex random variables with variance $\sigma^2$. The SNR for the $j$-th source is defined as

$$(SNR)_j = \frac{\sigma_j^2 \mathbf{s}_j^H \mathbf{s}_j}{4N\sigma^2}. \tag{12}$$

The correlation matrix $\mathbf{R}_{4N}$ is defined as

$$\mathbf{R}_{4N} = E[\mathbf{y}(t)\mathbf{y}(t)^H]. \tag{13}$$

In practical calculations, considering the received data is finite, the acoustic vector sensor array correlation matrix can be estimated as

$$\hat{\mathbf{R}}_{4N} = \frac{1}{L}\sum_{t=1}^{L}[\mathbf{y}(t)\mathbf{y}(t)^H], \tag{14}$$

where $L$ is the number of snapshots.

## 3 Compressive sampling

The concept of Compressive Sampling (CS) [2] is reviewed here. Compressive sampling is a sampling method used in the transform coding, which converts the input signals that are embedded in a high-dimensional space, into signals that lie in a space of significantly smaller dimensions. Examples of transform coders are wavelet transforms and the ubiquitous Fourier transform.

If $\mathbf{y} \in \mathbb{C}^N$ has a sparse representation in some orthonormal basis, then $\mathbf{y}$ can be represented as $\mathbf{y} = \mathbf{\Psi z}$, where $\mathbf{\Psi}$ is the $N \times N$ sparsity basis matrix and $\mathbf{z}$ is a $N \times 1$ vector with $K \ll N$ non-zero entries. The CS theory states that $\mathbf{y}$ can be recovered using $H = K\mathcal{O}(\log N)$ non-adaptive linear projection measurements on to an $H \times N$ random matrix $\mathbf{\Theta}$ that is incoherent with $\mathbf{\Psi}$ and that is usually over the field of real numbers. The measurement vector $\mathbf{y}_c$ can be written as

$$\mathbf{y}_c = \mathbf{\Theta y} = \mathbf{\Theta \Psi z}. \tag{15}$$

According to CS theory, the signal can be reconstructed using optimization strategies aimed at finding the sparsest signal that matches with the $H$ projections.

### 3.1 Benefits of compressive sampling on AVS array processing

Use of AVS array significantly reduces the number of sensors to achieve a given performance factor in the form of estimation error and bearing resolution. However, the analog signal conditioning hardware complexity and the data transmission rate increases by 4 times. The data transmission rate of the AVS array is given by

$$\text{Transmission-rate}_{\text{AVS}} = 4NF_sG \text{ bits/second}, \tag{16}$$

where $N$ is the number of AVS sensors, $F_s$ is the sampling frequency in Hz, $G$ is the number of bits/sample. Generally 16-bit or 24-bit sigma delta converters are used for digitization.

The above issues are efficiently tackled by the proposed compressive sampling or sensing receiver architecture. The proposed architecture uses only around $J \log(4N)$ analog front-end signal conditioning hardware and two bits of phase precision [16] instead of 16 or 24 bits. The data rate of the compressively sampled AVS array is given by

$$\text{Transmission-rate}_{\text{CS-AVS}} = J \log(4N) F_s 2 \text{ bits/second}, \tag{17}$$

where $J$ is the maximum number of expected acoustic sources.

CS array has the effect of compressing a large sized array into a smaller sized array. This in turn reduces the hardware complexity on account of the much smaller number of front-end circuit chains. Also, due to the smaller dimension of the array data vector, the software complexity is greatly reduced. The high resolution DoA estimation algorithms consist of inverse and eigenvalue decomposition of the spatial correlation matrix with computational complexity $\mathcal{O}(n^3)$ for an $n \times n$ matrix. The CS array architecture with CS beamformers needs to work with the correlation matrix $\hat{\mathbf{R}}_{y_c}$ of size $H \times H$ only, where $H \ll 4N$, while the conventional AVS array needs to work with $\hat{\mathbf{R}}_{4N}$ of size $4N \times 4N$. Figure 2 shows the block diagram of the CS-AVS array architecture. Table. 1 summarises the hardware requirement of the proposed CS-AVS array architecture and compares it with the conventional AVS array and scalar pressure sensor array.

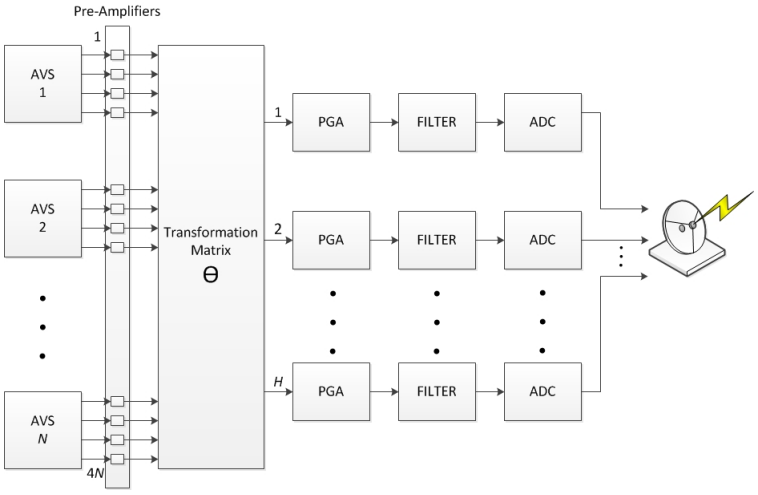


**Figure 2: Block diagram of the CS-AVS array architecture.**

**Table 1: Comparison of the different array architectures**

| Parameter | Scalar Sensor Array | AVS Array | CS-AVS Array |
|---|---|---|---|
| **No. of Channels** | $N$ | $4N$ | $J\log(4N)$ |
| **No. of signal conditioning hardware** | $N$ | $4N$ | $J\log(4N)$ |
| **Data rate (bits/sec)** | $NF_sK$ | $4NF_sK$ | $J\log(4N)F_s2$ |
| **Spatial Correlation Matrix** | $N \times N$ | $4N \times 4N$ | $J\log(4N) \times J\log(4N)$ |
| **Minimum number of snapshots** | $N$ | $4N$ | $J\log(4N)$ |

Note: The hardware requirement for the CS-AVS array is greatly reduced for large values of $N$ and $K$

It is clear that with greatly reduced complexity, the CS array can still achieve similar results in DoA estimation as a conventional large size AVS array.

### 3.2 Applying compressive sampling to the AVS array data model for shallow ocean.

On application of the compression matrix $\boldsymbol{\Theta}$ of size $H \times 4N$ to the original array signal vector $\boldsymbol{y}(t)$ of size $4N \times 1$, it is transformed to a compressed signal vector of size $H \times 1$

$$\mathbf{y}_c(t) = \boldsymbol{\Theta}\mathbf{y}(t). \tag{18}$$

The elements $\Theta_{h,n}$ of the compression matrix $\boldsymbol{\Theta}$ are drawn independently from a random distribution. If $\hat{J}$ is the expected number of sources, then we can take $H = \hat{J}\log(4N)$, so that embedding of the sparse signal into the compressed subspace $\boldsymbol{\Theta}$ does not destroy the essential information in the original signal.

Next, we compute the sample spatial correlation matrix $\hat{\mathbf{R}}_{y_c}$ of the compressed signal $\mathbf{y}_c$.

$$\hat{\mathbf{R}}_{y_c} = \frac{1}{L}\sum_{t=1}^{L}[\mathbf{y}_c(t)\mathbf{y}_c(t)^H], \tag{19}$$

where $L$ is the total number of time snapshots taken.

# 4 DoA estimation

## 4.1 Modified Subspace Intersection Method applied to CS-AVS Array

In this section, the subspace intersection method [14] is customized to suit the compressively sampled AVS array architecture. By applying an eigenvalue decomposition on the compressed sample spatial correlation matrix $\hat{\mathbf{R}}_{y_c} \in \mathbb{C}^{H\times H}$, we compute the eigen values and their corresponding eigen vectors. Construct the signal subspace using the eigen vectors corresponding to the higher $\hat{J}$ eigen values. The remaining $H - \hat{J}$ eigen vectors span the noise subspace. The number of sources $\hat{J}$ can be estimated using methods like Gerschgorin's disk method [17].

The compressed signal subspace $\mathbf{E}_c$ is then defined as

$$\mathbf{E}_c = \text{span}\{\mathbf{u}_{c_1}, \ldots, \mathbf{u}_{c_{\hat{J}}}\}, \tag{20}$$

where $\mathbf{u}_{c_1}, \ldots, \mathbf{u}_{c_{\hat{J}}}$ are the eigen vectors of $\hat{\mathbf{R}}_c$ corresponding to the $\hat{J}$ sources.

Now, the compressed modal subspace for the azimuth $\phi$ is defined as

$$\mathbf{M}_c(\phi) = \text{span}\{\mathbf{a}_c(\phi, k_1), \ldots, \mathbf{a}_c(\phi, k_M)\}, \tag{21}$$

where $\mathbf{a}_c(\phi, k_1), \ldots, \mathbf{a}_c(\phi, k_M)$ are the compressed modal steering vectors given by

$$\mathbf{a}_c(\phi, k_m) = \boldsymbol{\Theta}\mathbf{a}(\phi, k_m), \tag{22}$$

where $\mathbf{a}(\phi, k_1), \ldots, \mathbf{a}(\phi, k_M)$ are the modal steering vectors as defined in Eqs. (2-5).

We see that $\mathbf{E}_c$ and $\mathbf{M}_c(\phi)$ intersect only if a non-trivial linear combination of the linearly independent basis vectors of $\mathbf{E}_c$ and $\mathbf{M}_c(\phi)$ is a null vector.

Now, to estimate the DoA, we need to construct a $H \times (M + \hat{J})$ matrix $\mathbf{D}_c(\phi)$ defined as

$$\mathbf{D}_c(\phi) = [\mathbf{a}_c(\phi, k_1), \ldots, \mathbf{a}_c(\phi, k_M), \mathbf{u}_{c_1}, \ldots, \mathbf{u}_{c_{\hat{J}}}]. \tag{23}$$

The first $M$ columns of $\mathbf{D}_c(\phi)$ are the linearly independent basis vectors of the compressed modal subspace $\mathbf{M}_c(\phi)$ and the remaining $\hat{J}$ columns are the orthonormal basis vectors of the compressed signal subspace $\mathbf{E}_c$.

We now perform a $QR$ decomposition on $\mathbf{D}_c(\phi)$ so as to factorize $\mathbf{D}_c(\phi)$ as

$$\mathbf{D}_c(\phi) = \mathbf{Q}_c(\phi)\mathbf{R}_c(\phi). \tag{24}$$

Here,

$$\mathbf{Q}_c(\phi) = [\mathbf{q}_{c_1}(\phi), \ldots, \mathbf{q}_{c_{M+\hat{J}}}(\phi)], \tag{25}$$

is a $H \times (M + \hat{J})$ matrix whose columns $\mathbf{q}_{c_i}(\phi)$ are orthonormal vectors and $\mathbf{R}_c(\phi)$ is a $(M + \hat{J}) \times (M + \hat{J})$ upper triangular matrix with elements $r_{c_{ij}}(\phi)$.

The columns of $\mathbf{D}_c(\phi)$, denoted by $\mathbf{d}_{c_j}(\phi)$, are related to the columns of $\mathbf{Q}_c(\phi)$ through the equations

$$\mathbf{d}_{c_j}(\phi) = \sum_{i=1}^{j} r_{c_{ij}}(\phi) q_{c_i}(\phi), \tag{26}$$

for $j = 1, \ldots, M + \hat{J}$; hence,

$$\mathbf{d}_{c_j}(\phi) \in \text{span}\{q_{c_1}(\phi), \ldots, q_{c_{\hat{J}}}(\phi)\}. \tag{27}$$

If $\mathbf{d}_{c_j}(\phi) \in \text{span}\{\mathbf{d}_{c_1}(\phi), \ldots, \mathbf{d}_{c_{j-1}}(\phi)\}$, the diagonal element $r_{c_{jj}}(\phi)$ of the matrix $\mathbf{R}_c(\phi)$ is zero. It is this property that is utilised to estimate the DoA. The subspaces $\mathbf{M}_c(\phi)$ and $\mathbf{E}_c$ intersect only if $\phi \in \{\phi_1, \ldots, \phi_{\hat{J}}\}$. Therefore, $\phi \in \{\phi_1, \ldots, \phi_{\hat{J}}\}$ only if any one of the following conditions is satisfied:

- $\mathbf{d}_{c_j}(\phi) \in \text{span}\{\mathbf{d}_{c_1}(\phi), \ldots, \mathbf{d}_{c_M}(\phi)\}$, for $j \in [M + 1, \ldots, M + \hat{J}]$
- $\mathbf{d}_{c_{M+\hat{J}}}(\phi) \in \text{span}\{\mathbf{d}_{c_1}(\phi), \ldots, \mathbf{d}_{c_{M+\hat{J}-1}}(\phi)\}$

This implies that $\mathbf{d}_{c_j}(\phi) \in \text{span}\{\mathbf{d}_{c_1}(\phi), \ldots, \mathbf{d}_{c_{j-1}}(\phi)\}$ for $j \in [M+1, \ldots, M+\hat{J}]$ only if $\phi \in \{\phi_1, \ldots, \phi_{\hat{J}}\}$. As $r_{c_{jj}}(\phi)$ is zero only if $\mathbf{d}_{c_j}(\phi) \in \text{span}\{\mathbf{d}_{c_1}(\phi), \ldots, \mathbf{d}_{c_{j-1}}(\phi)\}$, it follows that $r_{c_{jj}}(\phi) = 0$ for some $j \in [M + 1, \ldots, M + \hat{J}]$ only if $\phi \in \{\phi_1, \ldots, \phi_{\hat{J}}\}$. Hence, the response function of the CS-SIM is given as

$$P_{CS-SIM}(\phi) = \left[ \min_{M+1 \le j \le M+\hat{J}} |r_{c_{jj}}(\phi)| \right]^{-1}. \tag{28}$$

### 4.2 Compressive beamforming

We estimate the angle pseudo-spectrum by modifying NM-MUSIC [12] for use with compressive sampled AVS array. Let $\mathbf{E}_{noise}$ be a matrix whose columns are the $H - \hat{J}$ noise eigenvectors of $\hat{\mathbf{R}}_{y_c}$. If we perform a one-dimensional scanning of the function $\mathbf{A}(\phi)$ along $\phi$, where $\mathbf{A}(\phi)$ is given by Eq. (2), we get $\hat{J}$ different $\mathbf{A}(\phi_j)$ (for j=1, ..., $\hat{J}$) which lie nearest to the signal sub-space. In compressive beamforming, we use $\mathbf{V}(\phi)$ instead of $\mathbf{A}(\phi)$, where

$$\mathbf{V}(\phi) = \Phi \mathbf{A}(\phi), \tag{29}$$

is the compressed array manifold matrix.

The projection of $\mathbf{V}(\phi)$ on the noise sub-space is given by

$$\text{projection} = \|\mathbf{V}(\phi)^H \mathbf{E}_{noise} \mathbf{E}_{noise}^H \mathbf{V}(\phi)\|_F, \tag{30}$$

where $||\bullet||$ denotes Frobenius norm. The estimated DoAs are given by

$$\phi_{CS-NM-MUSIC} = \arg\min_{\phi} \|\mathbf{V}(\phi)^H \mathbf{E}_{noise} \mathbf{E}_{noise}^H \mathbf{V}(\phi)\|_F. \tag{31}$$

Therefore, the spatial pseudo-spectrum estimate of NM-MUSIC is given by

$$P_{CS-NM-MUSIC}(\phi) = \frac{1}{\|\mathbf{V}(\phi)^H \mathbf{E}_{noise} \mathbf{E}_{noise}^H \mathbf{V}(\phi)\|_F^2}, \tag{32}$$

where $\phi = \phi_1, \ldots, \phi_{N_s}$ ($N_s$ is the total number of scanning angles).

Keeping the requirement of the MVDR [18], the pseudo-spectrum of the compressive sampling array can be derived similar to [12] and is given by

$$P_{CS-NM-MVDR}(\phi) = \frac{1}{\|\mathbf{V}(\phi)^H \mathbf{R}_{y_c}^{-1} \mathbf{V}(\phi)\|_F^2}. \tag{33}$$

Therefore, DoA estimation using compressive beamforming in shallow ocean using AVS array can be summarized as:

- Compute the spatial correlation matrix $\hat{\mathbf{R}}_{y_c}$ of the compressed signal $\mathbf{y}_c$ using Eqs. (18)-(19).
- Determine the eigenvectors corresponding to the $H - \hat{J}$ smaller eigenvalues of $\hat{\mathbf{R}}_{y_c}$ and form the $\mathbf{E}_{noise}$ matrix.
- Calculate $P_{CS-NM-MUSIC}(\phi)$ using Eq. (32) or $P_{CS-NM-MVDR}(\phi)$ using Eq. (33).
- Find the highest $\hat{J}$ peaks $P_{CS-NM-MUSIC}(\phi)$ or $P_{CS-NM-MVDR}(\phi)$
- The $\hat{J}$ azimuth angles corresponding to the peaks of $\mathrm{P}_{CS-NM-MUSIC}(\phi)$ or $\mathrm{P}_{CS-NM-MVDR}(\phi)$ are the DoA estimates of the $\hat{J}$ targets.

## 5 Results and discussions

In the simulations, we use Pekeris channel for modelling the horizontally stratified, range independent oceanic waveguide as detailed in section 2. The ocean depth is assumed to be 75 m. Sound speed in the water column is taken as 1500 m/s while that in the sediment is 1700 m/s. We assume an attenuation of 0.5 dB/wavelength. The density ratio of the sediment to that of the water is taken as 1.5. The source is fixed at 37.5 m and horizontal receiver array at 25 m from the top of the ocean. The compression matrix $\boldsymbol{\Theta}$ has entries drawn from an i.i.d Gaussian random process with mean= 0 and variance= $\frac{1}{H}$. Throughout the Monte-Carlo simulations, we use 200 snapshots or time samples ($L$=200) for the conventional AVS array and 20 for CS-AVS, unless otherwise stated, to demonstrate its superior strategic performance.

First, we compare the pseudo-spectrum performance of SIM, using 36 element conventional AVS array and the CS-AVS array ($N$=36, $H$=10) architecture. We consider two sources at 87° and 92° with respect to the array end-fire direction with 15dB SNR. Figure 3 shows the pseudo-spectrum response or SIM response function. Response of the 10-element conventional AVS array is also shown in Figure 3 for comparing the bearing resolution performance of SIM and CS-SIM using the same number of elements. It is seen that, (1) the performance of CS-AVS, which utilizes 10 measurements is not adversely affected in comparison with the conventional 36-element AVS array, consisting of 108 measurements, and (2) the conventional 10-element AVS array delivers a poor performance,

showing a prominent false alarm at the middle of the simulated targets. This clearly indicates the superior performance of the CS-AVS architecture which utilizes only 10.8% of the front-end signal conditioning hardware, and requiring only 2% data rate compared to the conventional AVS array configuration.

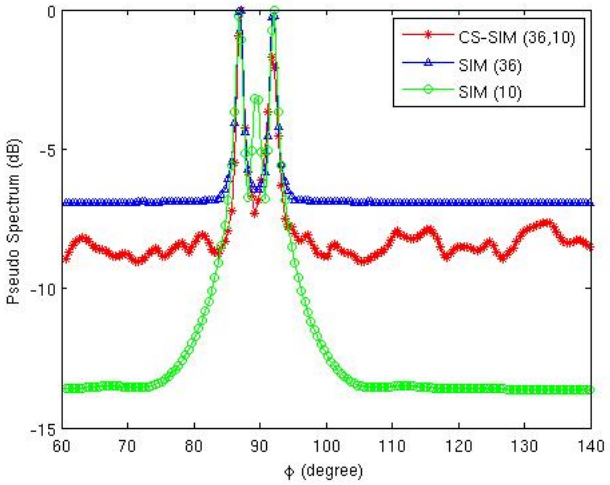


**Figure 3: SIM and CS-SIM pseudo-spectrum of the conventional AVS array ($N$=36, $L$=200), conventional AVS array ($N$=10, $L$=200) and the CS-AVS array ($N$=36, $H$=10, $L$=20). Two sources at $87^\circ$ and $92^\circ$. SNR=15 dB each, $f$=50 Hz.**

Figures 4 and 5 show, respectively, the plots of pseudo spectrum response of NM-MUSIC, NM-MVDR with the same source and array parameters used in the previous experiment. It shows that, (1) standard deviation or variance of the pseudo spectrum with respect to the source bearing, is large for CS algorithm compared to the conventional AVS array processing, (2) source signal level to the mean pseudo spectrum level is almost same for both conventional and CS algorithm and, (3) 10-element conventional AVS array has poor bearing resolution capability.

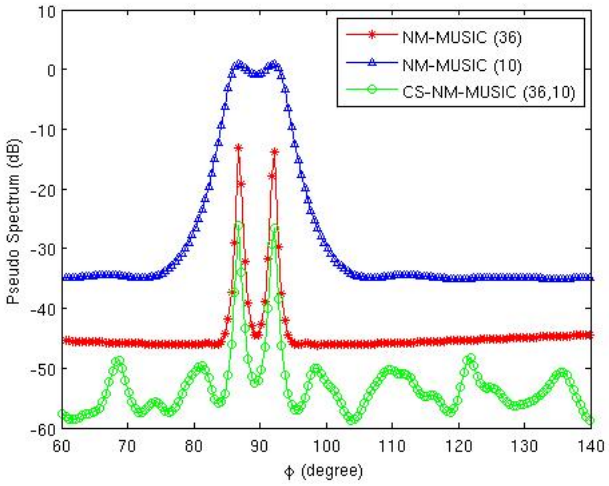


**Figure 4: NM-MUSIC pseudo-spectrum of the conventional AVS array ($N$=36, $L$=200), conventional AVS array ($N$=10, $L$=200) and the CS-AVS array ($N$=36, $H$=10, $L$=20). Two sources at $87^\circ$ and $92^\circ$. SNR=15 dB each, $f$=50 Hz.**

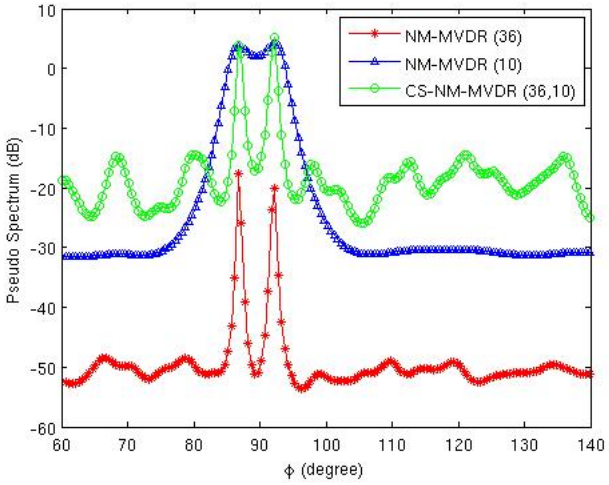


**Figure 5: NM-MVDR pseudo-spectrum of the conventional AVS array ($N$=36, $L$=200), conventional AVS array ($N$=10, $L$=200) and the CS-AVS array ($N$=36, $H$=10, $L$=20). Two sources at $87^\circ$ and $92^\circ$. SNR=15 dB each, $f$=50 Hz.**

Higher fluctuation in the CS methods are primarily due to the error in the estimation of the spatial correlation matrix using significantly reduced number of measurements and snapshots. It can be also viewed as a probabilistic reduction of signal entry into the reduced dimensional subspace. It is seen that, the conventional algorithm requires atleast $4N$ (i.e., $L \geq 4 \times 36 = 144$) snapshots, to compute the inverse of the spatial correlation matrix used in these algorithms. It is noteworthy that, in the conventional AVS array processing, higher bearing resolution is obtained by increasing the array aperture or increasing the number of sensors. It adversely affects the strategic performance of the system and also increases the size of the spatial correlation matrix. However, the CS-AVS processing ensures the

bearing resolution with minimum number measurements and hence achieves a high degree of strategic performance.

Figure 6 compares the pseudo-spectrum performance of SIM, using 36 element conventional AVS array with that of the CS-AVS array ($N$=36, $H$=10) architecture. We consider three sources at 30°, 35° and 60° with respect to the array end-fire direction and with 15 dB SNR. It is seen that, both conventional SIM and CS-SIM can resolve and localize two sources at 30° and 35°. However, it is noteworthy that, the hardware complexity of the proposed CS-SIM architecture is very less.

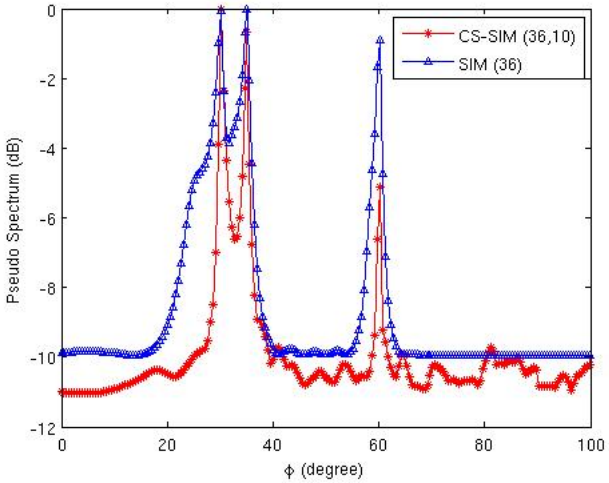


**Figure 6: SIM and CS-SIM pseudo-spectrum of the conventional AVS array ($N$=36, $L$=200) and the CS-AVS array ($N$=36, $H$=10, $L$=200). Three sources at $30°$, $35°$ and $60°$. SNR=15 dB each, $f$=50 Hz.**

The superior strategic performance of CS-SIM algorithm is demonstrated in Figure 7. We consider two sources at 87° and 92° with respect to the array end-fire direction with 15 dB SNR. The pseudo spectrum response function of CS-SIM is plotted with 2 snapshots or time samples ($L$=2). This experiment ensures the instantaneous attack time capability of the proposed CS-SIM architecture

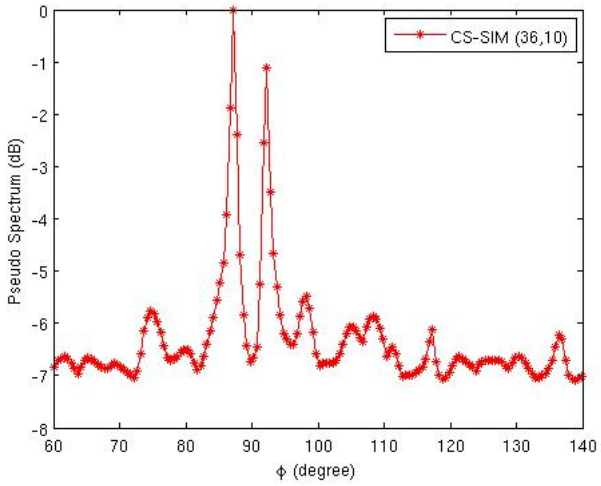


**Figure 7: CS-SIM pseudo-spectrum of the CS-AVS array ($N$=36, $H$=10, $L$=2). Two sources at $87^\circ$ and $92^\circ$. SNR=15 dB each, $f$=50 Hz.**

Figures 8 and 9 show, respectively, the plots of bias vs. bearing angle and root mean square error (RMSE) vs. bearing angle for a 36-element conventional AVS array along with that of the CS-AVS array ($N$=36, $H$=10) architecture. We use a single source with 0 dB SNR. It is seen that, the bias and the RMSE of the bearing estimate is slightly higher with CS-SIM, especially near the end-fire direction. It is also seen that, both in SIM and CS-SIM algorithm, the RMSE approaches CRB towards the broadside direction.

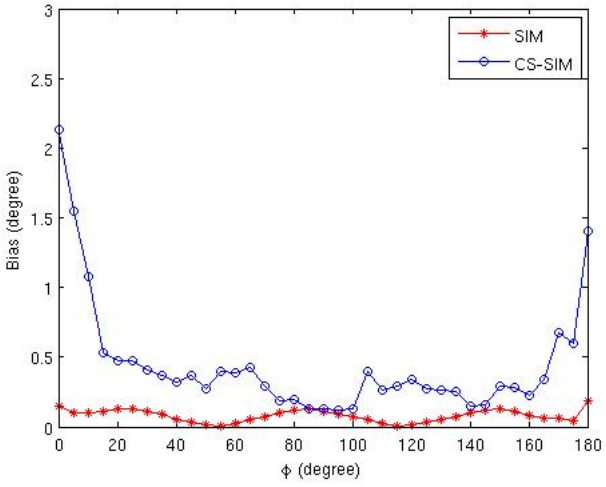


**Figure 8: Bias vs. source bearing of SIM and CS-SIM on the conventional AVS array ($N$=36, $L$=200) and the CS-AVS array ($N$=36, $H$=10, $L$=20). One source at $60^\circ$. SNR=0 dB, $f$=50 Hz.**

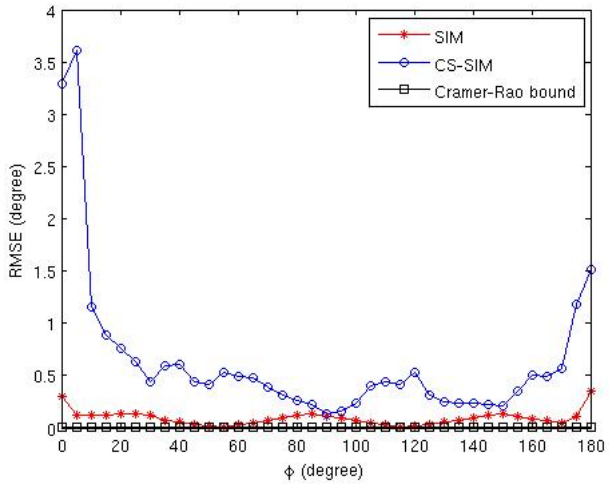


**Figure 9: RMSE vs. source bearing of SIM and CS-SIM on the conventional AVS array ($N$=36, $L$=200) and the CS-AVS array ($N$=36, $H$=10, $L$=20). One source at $60^\circ$. SNR=0 dB, $f$=50 Hz.**

Figures 10 and 11 show, respectively, the plots of bias vs. SNR and root mean square error (RMSE) vs. SNR of SIM and CS-SIM for a 36-element conventional AVS array along with with that of the CS-AVS array ($N$=36, $H$=10) architecture. For this experiment, we use a single source located at $60^\circ$. It is seen that, the bias and the RMSE of the bearing estimate is slightly higher with CS-SIM. It is also seen that, both in SIM and CS-SIM algorithms, the RMSE approaches CRB as SNR increases.

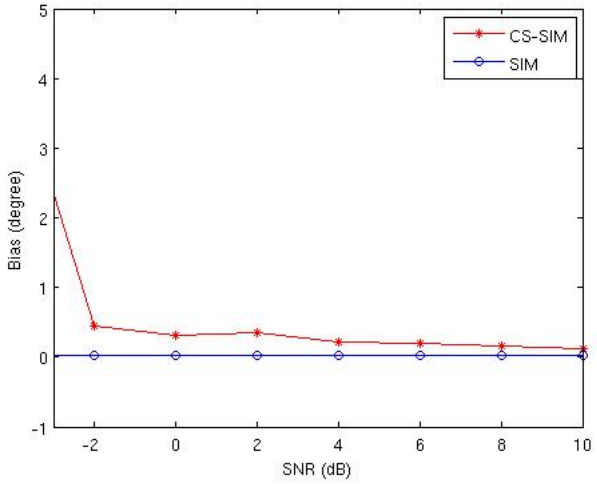


**Figure 10: Bias vs. SNR of SIM and CS-SIM on the conventional AVS array ($N$=36, $L$=200) and the CS-AVS array ($N$=36, $H$=10, $L$=20). One source at $60^\circ$, $f$=50 Hz.**

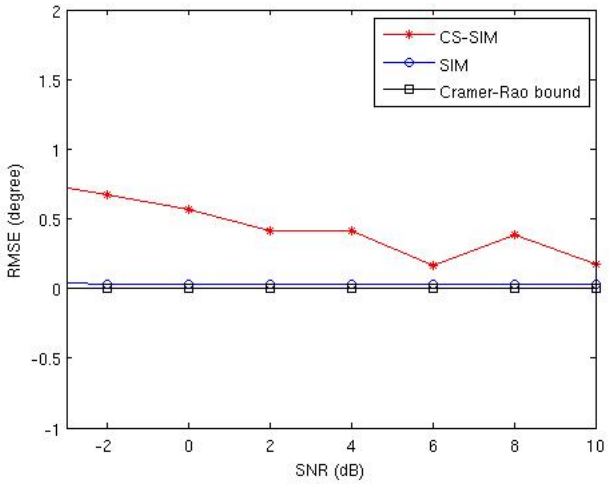


**Figure 11: RMSE vs. SNR of SIM and CS-SIM on the conventional AVS array ($N$=36, $L$=200) and the CS-AVS array ($N$=36, $H$=10, $L$=20). One source at $60^\circ$, $f$=50 Hz.**

Figures 12 and 13 show, respectively, the plots of bias vs. SNR and RMSE vs SNR of CS-SIM, CS-NM-MUSIC and CS-NM-MVDR for a 36-element CS-AVS array ($N$=36, $H$=10) architecture. A single source at 60° is used to compare the bias and RMSE performance of all the three high resolution angular spectral estimators in the compressive sampling framework. It is observed that, CS-SIM shows much better performance when compared with CS-NM-MVDR and CS-NM-MUSIC. For example, at -2 dB SNR, RMSE for CS-SIM is 0.5022 ° and the corresponding CRB is $0.1\times 10^{-3}$. This is primarily due to the inherent capability of SIM which uses both signal subspace and modal subspace to compute its response function.

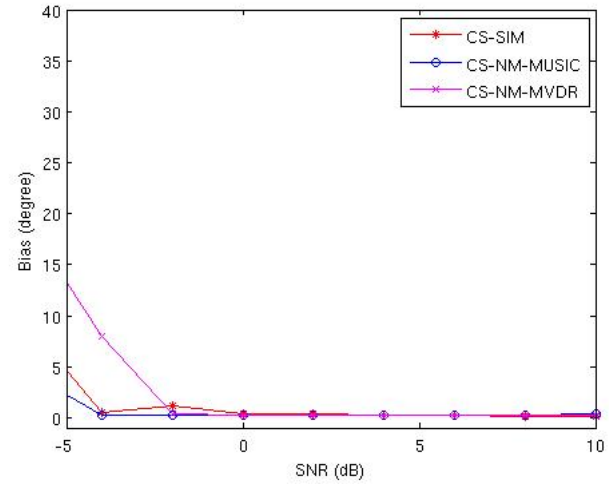


**Figure 12: Bias vs. SNR of CS-SIM, CS-NM-MUSIC and CS-NM-MVDR on the CS-AVS array ($N$=36, $H$=10, $L$=20). One source at $60^\circ$, $f$=50 Hz.**

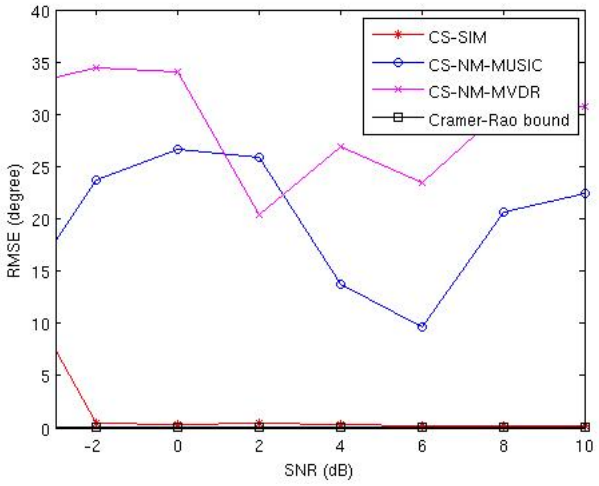


**Figure 13: RMSE vs. SNR of CS-SIM, CS-NM-MUSIC and CS-NM-MVDR on the CS-AVS array ($N$=36, $H$=10, $L$=20). One source at $60^\circ$, $f$=50 Hz.**

Figures 14 and 15 show, respectively, the plots of bias vs. number of snapshots and RMSE vs number of snapshots of CS-SIM, CS-NM-MUSIC and CS-NM-MVDR for a 36-element CS-AVS array ($N$=36, $H$=10) architecture. A single source at $60^\circ$ is used to compare the bias and RMSE performance of all the three high resolution angular spectral estimators. It is clear that, CS-SIM performs better with fewer snapshots when compared with CS-NM-MVDR and CS-NM-MUSIC.

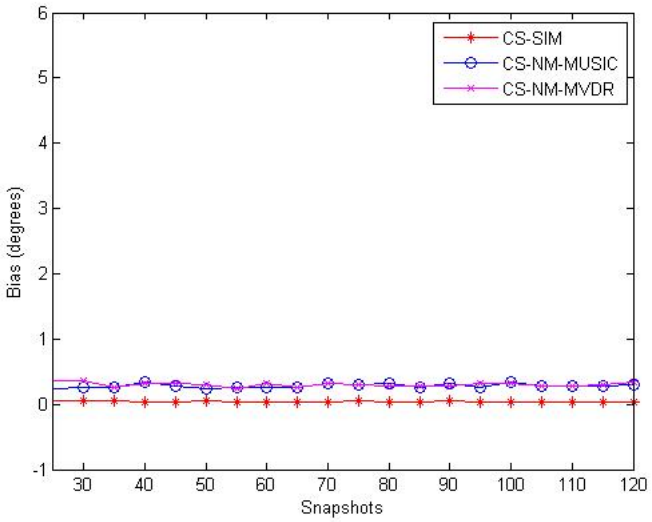


**Figure 14: Bias vs. snapshots of CS-SIM, CS-NM-MUSIC and CS-NM-MVDR on the CS-AVS array ($N$=36, $H$=10). One source at $60^\circ$. SNR=0 dB, $f$=50 Hz.**

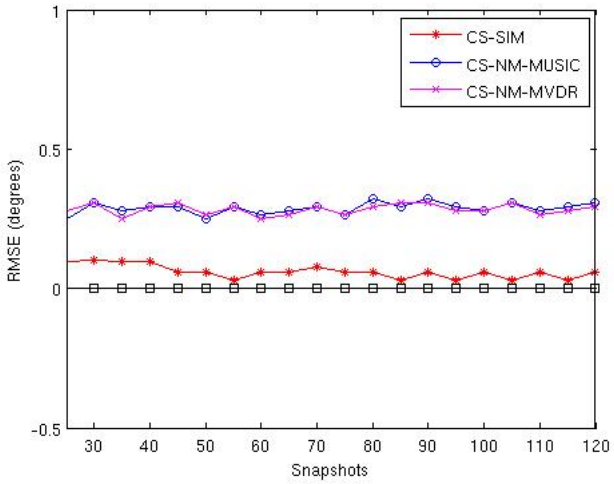


**Figure 15:** RMSE vs. snapshots of CS-SIM, CS-NM-MUSIC and CS-NM-MVDR on the CS-AVS array ($N$=36, $H$=10). One source at 60°. SNR=0 dB, $f$=50 Hz.

The significant hardware reduction capability of the proposed CS-SIM algorithm is shown in Figure 16. For this experiment, we use a single source located at 60° with 15dB SNR. The RMSE is computed by varying the number of channels or measurements ($H$). It is seen that, CS-SIM algorithm estimates the source bearing with a greater accuracy with minimum number of measurements. Superior performance of the CS-SIM in comparison with CS-NM-MVDR and CS-NM-MUSIC is mainly due to the fact that, signal localization is performed in both signal subspace and modal subspace.

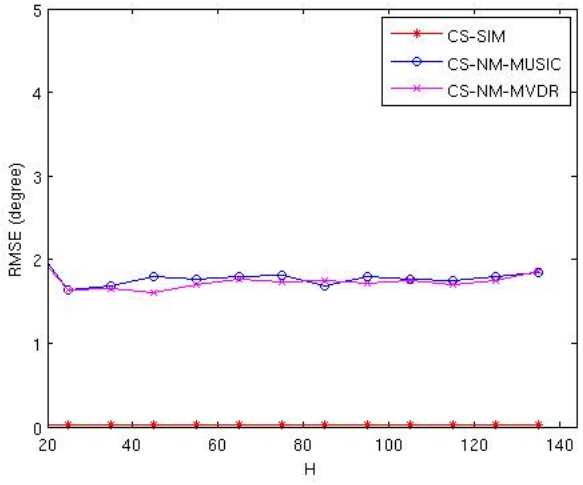


**Figure 16: RMSE vs. H of CS-SIM, CS-NM-MUSIC and CS-NM-MVDR on the CS-AVS array ($N$=36, $L$=144). One source at 60°. SNR=15 dB, $f$=50 Hz.**

## 6 Conclusions

In this paper, we have presented an economic, hardware efficient coastal surveillance architecture, capable for high resolution bearing estimation of multiple acoustic sources. The bearing angles are estimated using a one-dimensional search which does not require prior knowledge of sources ranges and depths. We have exploited the potential advantages of the inherent capabilities of acoustic vector sensor, compressed sensing and subspace intersection method. The high resolution shallow ocean spatial filtering techniques are modified to suit the compressively sensed AVS array. In this work, we have extensively reported the shallow ocean performance of high performance algorithms with and without compressive sensing. It is found that, the bias and RMSE performance of the high resolution techniques, NM-MVDR, NM-MUSIC shows highly inferior performance near the end fire direction in both the conventional and the compressive sampling framework. We have customized the SIM to suit the compressive sensing framework, and proved its superior performance with drastically reduced hardware. It is seen that the Cramer-Rao bound is of the order $10^{-4}$; CS-SIM achieves around $0.5022^{\circ}$ RMS error at -2 dB SNR while the high resolution estimators show much inferior performance.

## Acknowledgements

The authors express their gratitude to S. Ananthanarayanan, Director of NPOL, Kochi for his time and effort in reviewing the initial manuscript and providing valuable comments and suggestions.

## References

[1] A. Nehorai, E. Paldi, Acoustic vector-sensor array processing, IEEE Trans. Signal Process. 9, 42 **(1994)**

[2] David L. Donoho, Compressed Sensing, IEEE Trans. Inf. Theory 4, 52 **(2006)**

[3] E. Candes, J. Romberg, and T. Tao, Robust uncertainty principles: Exact signal reconstruction from highly incomplete Fourier information, IEEE Trans. Inf. Theory 2, 52 **(2006)**

[4] I. Daubechies, M. Defrise, and C. De Mol, An iterative thresholding algorithm for linear inverse problems with a sparsity constraint, Comm. Pure Appl. Math. 11, 57 **(2004)**

[5] M.A. T. Figueiredo, R. D. Nowak, and S. J. Wright, Gradient projection for sparse reconstruction: Application to compressed sensing and other inverse problems, IEEE J. Sel. Topics Signal Process, 4, 1**(2007)**

[6] Y.C. Pati, R. Rezaiifar, and P. S. Krishnaprasad, Orthogonal matching pursuit: Recursive function approximation with applications to wavelet decomposition. Proceedings of the 27th Asilomar Conference on Signals, Systems and Computers, **(1993)** November 1-3; Pacific Grove, CA

[7] S.G. Mallat and Z. Zhang, Matching pursuits with time-frequency dictionaries,IEEE Trans. Signal Process., 41, 12 **(1993)**

[8] A.C. Gilbert, M. J. Strauss, and R. Vershynin, One sketch for all: Fast algorithms for Compressed Sensing. Proceedings of the 39th ACM Symposium on Theory of Computing **(2007)** June 11-13; San Diego, CA

[9] M.A. Iwen, Combinatorial Sublinear-Time Fourier Algorithms, Foundations of Computational Mathematics 3, 10 **(2010)**

[10] Ali Cafer G*ürbüz*, James H. McClellan and Volkan Cevher , A Compressive Beamforming Method, Proceedings of the IEEE International Conference on Acoustics, Speech and Signal Processing **(2008)** March 31-April 4; Las Vegas, NV

[11] Ying Wang, Geert Leus and Ashish Pandharipande, Direction Estimation Using Compressive Sampling Array Processing, Proceedings of the IEEE/SP 15th Workshop on Statistical Signal Processing **(2009)** August 31-September 3; Cardiff, U.K

[12] Lijie Zhang, Jianguo Huang, Qunfei Zhang and Yunshan Hou, Normal-Mode Based MUSIC For Bearing Estimation In Shallow Water, Proceedings of the 5th IEEE Sensor Array and Multichannel Signal Processing Workshop **(2008)** July 21-23; Darmstadt, Germany

[13] Farida Akbari , Shahriar Shirvani Moghaddam, Vahid Tabataba Vakili, MUSIC and MVDR DOA estimation algorithms with higher resolution and accuracy, Proceedings of the 5th International Symposium on Telecommunications **(2010)** December 4-6; Tehran, Iran

[14] K.G. Nagananda, G.V. Anand, Subspace intersection method of high-resolution bearing estimation in shallow ocean using acoustic vector sensors, Els. J. Signal Processing 1, 90 **(2010)**

[15] N. Suresh Kumar, Soniya Peter, A. Unnikrishnan and C. Bhattacharya, Passive source localization using compressively sampled vector sensor array, accepted for publication in proceedings of the iMac4s **(2013)**, March 22-23; Kerala, India

[16] Dinesh Ramasamy, Sriram Venkateswaran, Upamanyu Madhow, Compressive Adaptation of Large Steerable Arrays, Proceedings of the Information Theory and Applications Workshop **(2012)** February 5-10; San Diego, CA

[17] N. Suresh Kumar, G. V. Anand, S. Roul and D. J. Philip, Source number estimation in shallow ocean by acoustic vector sensor array using Gerschgorin disks, 12th International Conference on System Design and Applications ISDA **(2012)**, November; Kochi, India
Hsien-Tsai Wu, Jar-Fen Yang, Fwu-Kuen Chen, Source Number Estimators Using Transformed Gerschgorin Radii, IEEE Trans. Signal Process., 6, 43 **(1992)**

[18] Harry L. Van Trees, Optimum Array Processing, Part IV Det., Est. and Mod. Theory, Wiley.

## Authors

**N. Suresh Kumar** is currently Scientist 'F', Naval Physical and Oceanographic Laboratory, Kochi, Kerala, India. He received his M.E degree in electrical communications from the Indian Institute of Science (IISc), Bangalore, India in 1995. His research areas include under water acoustics, sonar signal processing, compressive sensing and sensor networks.

**Dibu John Philip** is currently pursuing his M.Tech. degree in Signal Processing at the Mahatma Gandhi University, Kerala, India. His research interests include under water acoustics, machine learning and computer networks.

**A. Unnikrishnan** is currently Scientist 'H' (Outstanding Scientist), Naval Physical and Oceanographic Laboratory, Kochi, Kerala, India. He received his Ph.D from the Indian Institute of Science (IISc), Bangalore, India in 1988. His research interests include Sonar signal and information processing, machine learning, and image processing.

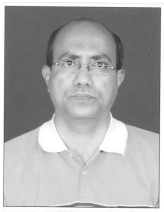

**C. Bhattacharya** heads the Dept. of Electronics Eng., Defence Institute of Advanced technology (DIAT), Pune, India. He is also a scientist 'F' with Defence Research and Development Organization. He received his Ph.D. from the Dept. of Computer Science and Engg., Jadavpur University, Kolkata in 2004. His research interests include synthetic aperture radar (SAR) signal and image processing, ultrawideband signals, stochatic processes, and bioiformatics. He is a senior member of the IEEE signal processing society, USA.